International Journal of Thermophysics, Vol. 10, No. 1, 1989

Theoretical Description of the Graphite, Diamond, and Liquid Phases of Carbon[1]

M. van Thiel[2] and F. H. Ree[2]

A three-phase equation-of-state model, to be used in high-pressure high-density simulations of systems containing carbon, is described for the system graphite–diamond–liquid. The solid phases are represented by cold lattice and thermal energy terms. Simple additivity of the energy terms is assumed and the cold curve is a modified Birch form. Liquid states for diamond and graphite are obtained by a previously described scaling model. The actual Gibbs free energy of the liquid state uses the free energy of these liquids in a mixture model that includes an entropy of mixing and a pressure-dependent strain term. It is noted that the thermal expansion coefficient and the Grüneisen gamma increase faster above 3000 K than the usual approximation for the volume dependence would predict. The result is a phase diagram that fits all available data.

KEY WORDS: carbon phases; diamond; electronic effects; graphite; melting; high pressure; high temperature.

1. INTRODUCTION

Carbon is both an excellent structural material and pervasive in nature. In high-temperature, high-pressure mixtures containing carbon, solid or liquid carbon can settle out as a separate phase [1] in an oxygen-deficient environment. The separate phase can be graphite, diamond, or liquid. An accurate three-phase model is therefore required to model such hot chemical equilibrium mixtures.

The status of the work on carbon has been reviewed recently [2, 3]. The graphite–diamond phase line is now well established to 3000 K and

[1] Paper presented at the Tenth Symposium on Thermophysical Properties, June 20–23, 1988, Gaithersburg, Maryland, U.S.A.

[2] Lawrence Livermore National Laboratory, Livermore, California 94550, U.S.A.

0195-928X/89/0100-0227$06.00/0

ends in a graphite–diamond–liquid triple point [4]. The uncertainty of this triple point temperature, 4000 to 4800 K, is due to the uncertainty of the low-pressure (about 0.01 GPa) graphite–liquid–gas triple point, to which it is connected by a distinctly curved melting line. The diamond melting line above the upper triple point was shown to be positive [5].

The electrical conductivity (or reflectivity) of liquid carbon depends on pressure [2, 4]. From the low-pressure triple point to about 0.5 GPa, the conductivity of the liquid appears to be similar to the conductivity of the solid or less conductive. But some disagreement exists on that point [2]. The liquid is generally more conductive than the solid at higher pressures. Aside from the conflict at low pressure, the data are consistent with a poorly conducting liquid below 0.1 GPa and an increasing conductivity with pressure.

2. THEORY

2.1. Solid

The solid state of the diamond and graphite phases is described assuming additivity of lattice and thermal terms:

$$E(T, V) = E_k(V) + \Delta E(V, T) + 0.5\, g_e T^2 \tag{1}$$

$$G(T, V) = E(T, V) - TS(T, V) - g_e T^2 + P(T, V)V \tag{2}$$

Here E is the internal energy and G the Gibbs free energy. T and V are temperature and volume, and the pressure (P) is the isentropic derivative of $-E$ with respect to V. The entropy (S) and thermal energy (ΔE) of the nuclear motions are evaluated in the Einstein approximation. The electronic corrections to the energy and Gibbs free energy, in their simple asymptotic forms, are adequate for the pressure (0.1- to 800-GPa) and temperature (0.05- to 5-eV) ranges considered.

The energy at 0 K, $E_k(V)$, is defined by a modified second-order Birch expansion [6] which is normalized to the heat of formation in the standard state (H_f^0) by its value (E_{0K}) at $V = V_0$. A second correction (δS_{298}) is used to correct the entropy at 298 K to the standard-state entropy. The modification of the Birch form is mandated by the high compressibility of the graphite lattice along the c axis and the strong bonding in the a, b plane, a condition for which no simple equation of state has been designed. For expanded states the Birch form is modified by

$$-\partial E_k/\partial(V_0/V) = P_{\text{BIRCH}}[(V_0/V)^2 + (V/V_0)^2]/2 \tag{3}$$

While this correction is important for graphite, it plays no role over the range of densities of significance for diamond.

We can express Eq. (1) as

$$P(V, T) = -[\partial E/\partial V]_S = P_0(V) + P_{T,I}(V, T) + P_{T,e}(T) \tag{4}$$

We use the Grüneisen approximation and write the last two terms as

$$P_{T,I}(V, T) = [\gamma_I(V)/V]\, \Delta E(V, T) \tag{5a}$$

$$P_{T,e}(V, T) = (\gamma_e/2V)\, g_e T^2 \tag{5b}$$

The above approximation is synonymous with the assumption that all vibrational modes of the system have the same volume dependence and the volume dependence of the Einstein Θ is, therefore, $\partial \ln \Theta/\partial \ln V = -\gamma_I$. Its value at $V = V_0$ is defined by the experimental heat capacity.

The solid is bounded at high T by the melting line. The Lindemann law in its usual harmonic approximation, $\Theta^2 V_m^{2/3}/T_m = \text{constant}$, leads to the melting law [7],

$$\partial \ln T_M/\partial \ln V = \lambda = 2\gamma_I - 2/3 \tag{6}$$

At this point the melting line is independent of the electronic properties. This will change as we develop the liquid properties of the graphite–diamond system below.

As discussed below, the expansion coefficient appears to have a larger curvature above 3000 K. The following expression can describe fairly rapid changes in curvature:

$$\gamma_I(V)/V = \gamma_0/V_0[1 + \delta_{1\gamma}(1 + \tanh Z_1) + \delta_{2\gamma}(1 + \tanh Z_2)] \tag{7a}$$

where

$$Z_i = \pm(V - V_{i\gamma})/\delta V_{i\gamma}, \qquad \text{with} \quad i = 1 \text{ or } 2 \tag{7b}$$

2.2. Liquid

Experimental data and theoretical considerations indicated that the atomic heat capacity of the liquid, $C_{V,L}$, is related to the solid heat capacity, C_V, by

$$C_{V,L} = C_V - \frac{3}{2} R \frac{\alpha\tau}{(1 + \alpha\tau)} \tag{8}$$

with $\alpha = 0.1$. Grover [7] has shown that with this rule the liquid equation

of state can be determined from the properties of the solid and the melting line by a thermodynamically consistent scaling procedure. We have applied this formalism to define graphitic and diamond-like liquid phases.

The liquid state is now defined by two Gibbs free energies, one for diamond and another for graphite; these produce a first-order transition in the liquid. There is no evidence for such a transition in simple liquids. Furthermore, fluctuations in interatomic distance in the liquid phase can readily lead to diamond-like tetrahedral sites with a probability that increases with compression. This view is supported by structural analysis of flash-frozen droplets [8], and the low activation energy for diamond formation of rhombohedral graphite [9]. We therefore treat the liquid, as in a previous more approximate analysis [10], as a solution of two liquids. Solution theory [11] gives the Gibbs free energy

$$G_{\mathrm{L}}(V, T) = xG_{d,\mathrm{L}}(V, T) + (1-x)\, G_{\mathrm{g},\mathrm{L}}(V, T) + RT[x \ln x + (1-x)\ln(1-x) + A(P)\, x(1-x)] \tag{9}$$

where subscripts L, d, and g refer to liquid, diamond, and graphite, respectively. The logarithmic terms are the entropy of mixing and A is the strain energy. This term is included because there is a boundary of molecules between graphitic and diamond-like sites that accommodates the strain caused by the difference in size. Choice of a constant A yields reasonable results. The results are improved by a pressure-dependent expression:

$$A(P) = A_0/[1 + (P/P_0)^{1.5}] \tag{10}$$

3. ANALYSIS AND RESULTS

The high-temperature heat capacity of graphite and diamond are easily reproduced by Einstein functions. Deviations near and below room temperature can be corrected. The reference energy ($E_{0\mathrm{K}}$) in the Birch form of $E_k(V)$, Eq. (1), and the entropy correction (δS_{298}) have been discussed above. With these constants, the computed graphite–diamond transition agrees with experiment [2].

The bulk modulus of diamond can be determined from existing shock-wave and ultrasonic data, but a good guide is provided by first-principles calculations. In Fig. 1a several sources of data are compared to our model Hugoniot and 0 K isotherm. The data analysis of Pavlovski [12] ignored strength effects. But Kondo and Ahrens [13] measured an elastic precursor of about 60 GPa. The Pavlovski data were recalculated with this precursor pressure. The limits of uncertainty in the measured shock and particle velocities yield a number of points per datum. These are all plotted in

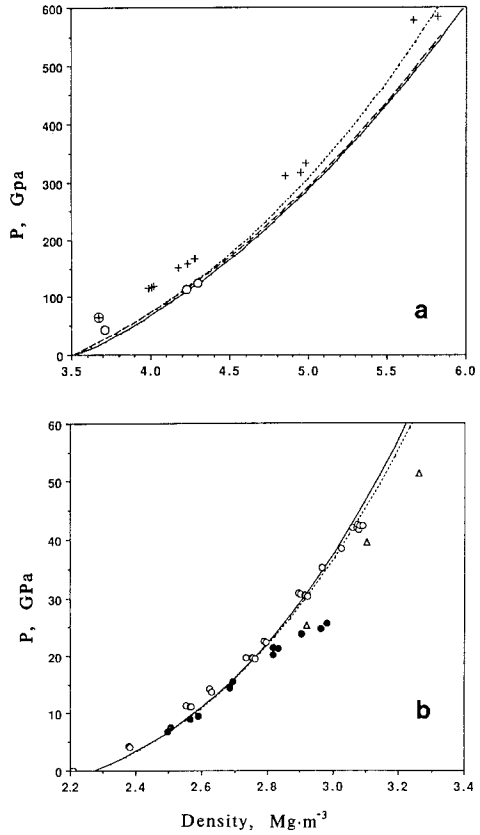

Fig. 1. (a) Diamond. 0 K isotherms: (——) McMahan's [15] LMTO calculations; (----) this model. Hugoniots: (----) this model; (+) Pavlovski [12]; (○) McQueen et al. [14]; (⊕) Kondo and Ahrens [13]. (b) Graphite. 0 K isotherms: (△) Fahy's rhobohedral graphite [21]; (——) this model. Hugoniots: (——) this model; (○) pyrolytic; (●) pressed powder.

Fig. 1a to offer a measure of the uncertainty. Several data points obtained on pressed diamond powder with a graphite binder [14] yield a higher density. Since the shock develops most of the temperature in the binder, the stress field in this sample should be considerably more hydrostatic. This is consistent with the higher shock densities of the powder data and their close agreement with the results from LMTO calculations [15]. The selected bulk modulus, B_0, and its pressure derivative, B_0', produce close

agreement with the theoretical calculations. The bulk modulus also agrees with existing ultrasonic data within experimental uncertainty.

The weak binding between the a, b planes makes the compressibility of graphite near $P=0$ very nonlinear. As noted above, the second-order Birch equation requires a correction in expansion. Ultrasonic data up to 40 MPa [16] show that $\partial B_0/\partial P = 33$, while static compression work [17] up to 18 GPa suggests a value of 7 to 9. The shock-wave data of pyrolytic graphite [14] to 40 GPa imply a value of 7.2. The pyrolytic shock data have slightly high pressures up to 18 GPa, which could be a consequence of sample porosity. Strength effects have been ignored in matching the shocked pyrolytic data near 40 GPa. This is supported by the near-equality of the one-dimensional and bulk compression moduli obtained from low-pressure elastic constants. Extrapolation of this equality to high pressure may not be justified.

The shock data of pressed graphite powders have higher densities above 10 GPa than the data of pyrolytic graphite. However, shock compression of these powders can produce rather high transient temperature spikes (on a micron scale) between the grains, high enough to produce partial transformation to diamond. Calculations also show that in the rhombohedral form the graphite in-plane bonds bend, thereby allowing stronger bonding between the planes [9]. This structure is easily formed in polycrystalline samples because of the random orientation of the particles relative to the principal stress direction. Tetrahedral structures with a higher density are therefore more likely in such randomly oriented polycrystalline samples. Such samples are therefore not a useful measure of the compressibility of crystalline graphite. It may also be noted at this point that the value of B_0' for graphite in Table I, within parentheses, is appropriate for expanded states where a large value does not give meaningful results in the Birch form.

The thermal effects may be estimated from the expansion coefficient and the selected moduli. For diamond the expansion coefficient is known only to 1200 K and yields a value of $\gamma_0 = 0.86$. The best estimate of its value at high pressure comes from data above 400 GPa [18]. These data suggest a γ_0 of 1.15. We have adopted the latter value since our interest is in the high pressures where diamond is stable.

Expansion data for graphite extend to 3000 K, nearly three times Θ_E. Combined with the low modulus of graphite, this yields, a small value of γ ($=0.35$), and resulting pressure differences between the 0 K curve in Fig. 1b and the Hugoniot are, therefore, also small. The unusual form for γ in Eq. (7) is dictated by the value required to explain the positive slope of the graphite melting line at low pressures [4]. This implies a rapidly increasing expansion coefficient between 3000 K and the melting point. The

Table I. Input Constants for the Model[a]

	E_{0K}/R (K)	γ_0	γ_e	$\gamma_{e,L}$
Graphite	−53.3015	0.35	0.24	0.24
Diamond	190.2730	1.15	1.10	1.10
	θ_E (K)	g_e/R (K^{-1})	$g_{e,L}/R$ (K^{-1})	$T_{M,0}$ (K)
Graphite	1280.	1.156×10^{-6}	1.156×10^{-6}	6000
Diamond	1411.	0.0	6.038×10^{-5}	6600
	$\Delta S_M/R$	B_0 (Mbar)	B_0'	$\delta S_{298}/R$
Graphite	2.70	0.511	7.2 (5.0)[b]	0.464
Diamond	1.15	4.397	3.65	0.1331
	$\delta_{1\gamma}$	$\delta_{2\gamma}$	$\delta V_{1\gamma}$ ($cm^3 \cdot g^{-1}$)	$\delta V_{2\gamma}$ ($cm^3 \cdot g^{-1}$)
Graphite	0.10	3.0	0.040	0.065
Diamond	0.0	0.0	1.0	1.0
	$V_{1\gamma}$	$V_{2\gamma}$	A_0	P_0 (GPa)
Graphite	0.500	0.22		
Diamond	0.0	0.0		
Liquid			2.2	20.

[a] $R = 82.05586$ atm $\cdot$ $cm^3 \cdot mol^{-1} = 6.92215 \times 10^{-6}$ Mbar $\cdot$ $cm^3 \cdot g^{-1}$.
[b] The value in parentheses is used in expansion.

high rate of graphitization [19] and the possibility of forming carbynes [20] above 2600 K imply that the in-plane lattice motions are quite anharmonic in this temperature range.

The electronic properties of graphite are reflected in measurements of the conductivity and low-temperature heat capacity. The measurements of Bundy [4] show a decrease in conductivity with temperature, consistent with the semimetal band structure of the static lattice, and an increase on liquefaction. As noted above, the increase of the conductivity on melting occurs only above 0.4 GPa. For the range of pressures and temperatures of interest here, we assume that the band structure and electronic heat capacity coefficient for solid graphite and the liquid graphite component are constant. Low-temperature heat capacity measurements yield the electronic value listed in Table I.

The conductivity of diamond is structure dependent. The normal cubic

diamond structure is easily transformed to hexagonal diamond in a shock wave. While the former remains an insulator at high pressure, the hexagonal form has a band gap, which decreases to about 1.5 eV at 300 GPa [21]. Bundy had noticed that doped liquid diamond is more conductive than the solid [4]. For most dynamic experiments that produce a liquid state, the temperatures would be sufficiently high to yield a conductor of disordered hexagonal diamond. Calculations using the INFERNO (atom in a Wigner–Seitz sphere) model [22] indicate that, for equation-of-state purposes, the electronic heat capacity can be represented by $g_e T$ and γ_e by a constant. In this model we have used the electronic properties derived from INFERNO for the liquid and assumed only bound electrons in the generally cooler solid.

The phase diagram in Fig. 2 fits the known information within experimental uncertainty. The agreement with the graphite–diamond transformation data of Berman and Simon [23] and Bundy et al. [24] has been reported previously [25]. The principal improvement obtained in this work is in the melting properties. Near 1 GPa our mixture model predicts about 90% graphitic liquid. The amount of diamond-like liquid increases only slowly with pressure up to 3 GPa, then more rapidly, and tends to

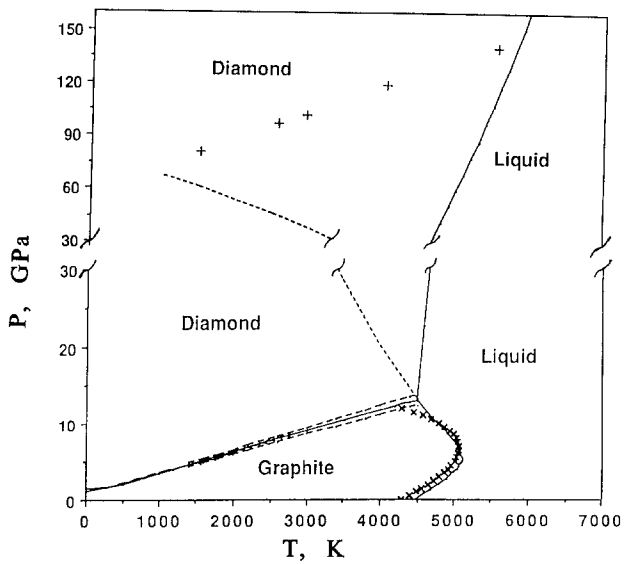

Fig. 2. Carbon phase diagram: (×) Bundy's experimental melting line [4]; (---) Berman and Simon [23]; (——) this model; (----) graphite melting line extension, this model; (+) solid Hugoniot points, Shaner et al. [5].

level off at about 80% just above the triple point. The slope of the melting line above 5 GPa is, therefore, a function of the diamond fraction and A in Eq. (10). A pressure-dependent A, using the constants in Table I, lowers dP_M/dT by about a factor of 2 over that obtained with a constant value of A. The small negative slope, therefore, results both from the increasing tetrahedral character of the liquid and from the decreasing strain energy with pressure.

The diamond melting line in this work has a positive slope, which is consistent with the high-pressure sound-speed measurements of Shaner et al. [5]. These measurements determined the Poisson ratio of the shocked material and showed that all points are in the solid phase. The model presented here places the melting line close to the highest-pressure point in Fig. 2. The extension of the graphite melting line and, to a lesser extent, the diamond melting line depends on the compressibility of the unstable graphite phase. This compressibility is constrained by experiment only up to 40 GPa. Extrapolation of the melting line is often used as a criterion of instability. Our extrapolation would predict graphite to be stable up to 80 GPa, which is also predicted by local density functional theory [9] of rhombohedral graphite.

4. CONCLUSION

We have combined a simple description for the high-pressure and -temperature properties of solid graphite and diamond with a description of the liquid phase. The observed curvature of the graphite melting line requires a new function for the Grüneisen γ and a mixture model for the liquid. The positive slope of the diamond melting line also is consistent with the available experimental data. If we consider the extrapolation of the grahite melting line as the curve bounding its range of stability, we note agreement with the theoretical stability range of rhombohedral graphite.

ACKNOWLEDGMENTS

This work was performed under the auspices of the U.S. Department of Energy by the Lawrence Livermore National Laboratory under Contract 7405-ENG-48. We greatly appreciate the support of Dick Grover during the development of this model and the discussions with David Young. Andy McMahan supplied us with his theoretical diamond data. We also appreciate the support of G. Kerley, B. I. Bennett, and D. A. Liberman with the INFERNO calculations. Our discussions with Drs. F. P. Bundy, S. Fahy, J. Shaner, A. Cezairliyan, and A. P. Miiller have improved our understanding of the characteristics of carbon.

REFERENCES

1. M. van Thiel and F. H. Ree, *J. Appl. Phys.* **62**:1761 (1987).
2. F. P. Bundy, *Proc. XI AIRAPT Int. Conf.*, Kiev, USSR, July 1987 (in press).
3. P. Gustafson, *Carbon* **24**:169 (1986).
4. F. P. Bundy, *J. Chem. Phys.* **38**:618, 631 (1963).
5. J. W. Shaner, J. M. Brown, C. A. Swenson, and R. G. McQueen, *J. Phys.* **45** (Suppl.):C8-235 (1984).
6. D. L. Anderson, *Phys. Earth Planet. Inter.* **1**:169 (1968).
7. R. Grover, *Proceedings of the Seventh Symposium on Thermophysical Properties*, A. Cezairliyan, ed., (Am. Soc. Mech. Eng., New York, 1977).
8. M. S. Weathers and W. A. Bassett, *Phys. Chem. Minerals* **15**:105 (1987).
9. S. Fahy, S. G. Louie, and M. L. Cohen, *Phys. Rev.* **B34**:1191 (1986).
10. I. A. Korsunskaya, D. S. Kamenetskaya, and I. L. Aptekar', *Fiz. Metal. Metalloved.* **34**:39 (1972).
11. E. Rapoport, *J. Chem. Phys.* **46**:2891 (1967).
12. M. N. Pavlovskii, *Soviet Phys.-Solid State* **13**:741 (1971).
13. K. Kondo and T. J. Ahrens, *Geophys. Res. Lett.* **10**:281 (1983).
14. M. van Thiel (ed.), *Compendium of Shock Wave Data, Vol. 1* (NTIS, NBS, Springfield, VA., 1977), p. 31 ff.
15. A. K. McMahan, *Phys. Rev.* **B30**:5835 (1984).
16. O. L. Blakslee, D. G. Proctor, E. J. Seldin, G. B. Spence, and T. Weng, *J. Appl. Phys.* **41**:3373 (1970).
17. H. G. Drickamer, R. W. Lynch, E. L. Clendenen, and E. A. Perez-Albuerne, *Solid State Phys.* **19**:135 (1966); M. Hanfland, H. Beister, and K. Syassen, Private communication, Max-Plank-Institut, Stuttgart, Germany (1988).
18. W. J. Nellis and A. C. Mitchell, Private communication, Lawrence Livermore National Laboratory, Livermore, Calif.
19. E. Fitzer and M. Heym, *High Temp.-High Press.* **10**:29 (1978).
20. A. G. Whittaker, *Nature* **267**:695 (1978).
21. S. Fahy and S. G. Louie, *Phys. Rev.* **36B**:3373 (1987).
22. D. A. Liberman, *Phys. Rev.*. **B20**:4981 (1979).
23. R. Berman and Sir Francis Simon, *Z. Elektrochem.* **59**:333 (1955).
24. F. P. Bundy, H. P. Bovenkerk, H. M. Strong, and R. H. Wentorf, Jr., *J. Chem. Phys.* **35**:383 (1961).
25. M. van Thiel, F. H. Ree, and R. Grover, *Shock Waves in Condensed Matter*, S. C. Schmidt and N. C. Holmes, eds. (Elsevier, Amsterdam, 1988), p. 81.